Chest radiographic findings of pulmonary tuberculosis in severely immunocompromised patients with the human immunodeficiency virus

[1]H N KISEMBO, MMed, MPH, [2]S DEN BOON, MSc, PhD, [3]J L DAVIS, MD, MAS, [4]R OKELLO, MBChB, MMED, [5]W WORODRIA, MBChB, MMed, [3]A CATTAMANCHI, MD, MAS, [3]L HUANG, MD, MAS and [4]M G KAWOOYA, MED, PHD

[1]*Department of Radiology, Mulago National Referral Hospital, Kampala, Uganda,* [2]*Makerere University–University of California, San Francisco (MU-UCSF) Research Collaboration, Kampala, Uganda,* [3]*Division of Pulmonary and Critical Care Medicine, University of California, San Francisco, CA, USA,* [4]*Department of Radiology, Makerere University, Kampala, Uganda, and* [5]*Department of Internal Medicine, Makerere University, Kampala, Uganda*

Objective: We describe chest radiograph (CXR) findings in a population with a high prevalence of human immunodeficiency virus (HIV) and tuberculosis (TB) in order to identify radiological features associated with TB; to compare CXR features between HIV-seronegative and HIV-seropositive patients with TB; and to correlate CXR findings with CD4 T-cell count.

Methods: Consecutive adult patients admitted to a national referral hospital with a cough of duration of 2 weeks or longer underwent diagnostic evaluation for TB and other pneumonias, including sputum examination and mycobacterial culture, bronchoscopy and CXR. Two radiologists blindly reviewed CXRs using a standardised interpretation form.

Results: Smear or culture-positive TB was diagnosed in 214 of 403 (53%) patients. Median CD4+ T-cell count was 50 cells mm^{-3} [interquartile range (IQR) 14–150]. TB patients were less likely than non-TB patients to have a normal CXR (12% *vs* 20%, $p=0.04$), and more likely than non-TB patients to have a diffuse pattern of opacities (75% *vs* 60%, $p=0.003$), reticulonodular opacities (45% *vs* 12%, $p<0.001$), nodules (14% *vs* 6%, $p=0.008$) or cavities (18% *vs* 7%, $p=0.001$). HIV-seronegative TB patients more often had consolidation (70% *vs* 42%, $p=0.007$) and cavities (48% *vs* 13%, $p<0.001$) than HIV-seropositive TB patients. TB patients with a CD4+ T-cell count of $\leq$50 cells mm^{-3} less often had consolidation (33% *vs* 54%, $p=0.006$) and more often had hilar lymphadenopathy (30% *vs* 16%, $p=0.03$) compared with patients with CD4 51–200 cells mm^{-3}.

Conclusion: Although different CXR patterns can be seen in TB and non-TB pneumonias there is considerable overlap in features, especially among HIV-seropositive and severely immunosuppressed patients. Providing clinical and immunological information to the radiologist might improve the accuracy of radiographic diagnosis of TB.

Received 5 July 2010
Revised 15 October 2010
Accepted 18 October 2010

DOI: 10.1259/bjr/70704099

Respiratory infections, especially tuberculosis (TB), are leading causes of illness and death in human immunodeficiency virus (HIV)-infected patients in sub-Saharan Africa. Rapid and accurate diagnosis of the specific cause of infection has the potential to reduce mortality substantially [1, 2]. Although sputum smear microscopy for acid-fast bacilli (AFB) is the first-line diagnostic test for evaluating these patients, chest radiographs (CXRs) are recommended for patients with negative sputum smears [3]. Studies have shown that HIV-infected patients with pulmonary TB are less often smear-positive and tend to have less ''typical'' radiographic abnormalities, two factors which make TB diagnosis even more difficult than in HIV-seronegative patients [4–6].

Although the clinical and radiological manifestations of TB in HIV-infected patients are known to vary according to the degree of immunosuppression [7–13], no studies have specifically described radiographic abnormalities in patients with CD4+ T-cell counts below 50 cells mm^{-3}, a population at particularly high risk of poor outcomes. Therefore, we carried out a cross-sectional study of adult patients admitted to the emergency ward of a national referral hospital with suspected TB. We describe CXR findings among this population with a high prevalence of HIV and TB in order to identify radiological features that could identify TB; we compare radiographic features between HIV-seronegative and HIV-seropositive patients with TB; and we correlate CXR findings of TB with CD4+ T-cell counts.

Address correspondence to: Dr Harriet Kisembo, Department of Radiology, Mulago National Referral Hospital, PO Box 7051, Kampala, Uganda. E-mail: kisemboharriet@yahoo.co.uk

Methods and patients

Study population

Between September 2007 and July 2008, we screened all adult patients admitted to the medical emergency ward with a cough of duration of 2 weeks or longer but less than 6 months. Patients already receiving therapy for TB were excluded, as were patients who were unwilling or unable to consent in English or a local language.

Data collection

After obtaining written informed consent, medical officers administered a standardised questionnaire to collect demographic and clinical information. Laboratory technicians collected blood samples for HIV testing using whole blood fingerstick specimens according to a sequential testing algorithm incorporating three rapid enzyme immunoassay kits, Determine (Abbott Laboratories, Abbott Park, IL), Stat-Pak (Chembio, Medford, NY) and Uni-Gold (Trinity Biotech, Wicklow, Ireland). CD4+ T-lymphocyte counts were measured in all HIV-infected patients.

All study participants provided spot sputum on hospital day 1 and early-morning sputum on hospital day 2. Patients who were unable to produce a sample underwent sputum induction with nebulised hypertonic saline according to routine procedures practised on the pulmonary ward. Specimens were examined by direct Ziehl–Neelsen (ZN) smear microscopy and mycobacterial culture on Löwenstein–Jensen (LJ) medium. Cultures were read weekly for growth, and were considered negative if no growth was seen after 8 weeks.

The study team referred all HIV-infected patients with negative sputum smears for AFB for bronchoscopy, except when the clinicians deemed it unsafe, which clinical investigators (WW, SY, AC, JLD) performed according to a standardised protocol that included airway inspection for Kaposi's sarcoma lesions and collection of bronchoalveolar lavage (BAL) fluid.

Trained microbiology technicians examined BAL fluid for mycobacteria (smear and culture), *Pneumocystis jirovecii* (modified Giemsa stain) and other fungi (potassium hydroxide stain and culture on Sabouraud's agar). We provided all test results to treating physicians to be used in patient management as soon as the results were available.

We invited patients to return 2 months after enrolment for a follow-up clinical examination and repeat sputum analysis, if clinically indicated. After participants had completed study procedures and the 2 month follow-up visit, at least two pulmonary physicians (SY, WW, AC, JLD and LH) reviewed all available clinical and microbiological data and assigned final diagnoses according to explicit definitions as follows: (1) culture-positive TB, positive sputum or BAL fluid mycobacterial culture results; (2) smear-positive, culture-negative TB, positive sputum AFB smear but negative mycobacterial cultures; (3) fungal pneumonia, positive BAL fluid fungal culture; (4) pulmonary Kaposi's sarcoma (PKS), observation of typical violaceous lesions of the tracheal and bronchial mucosa at bronchoscopy or violaceous plaques of the skin or mucous membranes; (5) cryptococcal pneumonia, positive BAL culture for *Cryptococcus*; (6) *Pneumocystis jirovecii* pneumonia (PCP), positive BAL fluid Giemsa stain; (7) aspergillus pneumonia, positive BAL culture for *Aspergillus*; (8) bacterial pneumonia, a diagnosis of exclusion, *i.e.* no alternative diagnosis and clinical diagnosis of bacterial pneumonia and clinical response to treatment at 2 months and all AFB cultures negative; (9) others, an infectious illness not mentioned above or any non-infectious illness that explained all of the pulmonary symptoms; (10) unknown, the patient did not meet any of the criteria above.

Chest radiographs

A hospital radiographer performed baseline postero-anterior (PA) or anteroposterior (AP) (in patients who were unable to stand) chest radiography within 24 h of admission. If a patient had had a CXR within the previous 7 days, it was not repeated. Study personnel photographed the CXRs using a 4.1 mega-pixel digital camera according to a standardised protocol.

Two radiologists (HNK, MGK), certified by the National Medical Association Board and each with more than a decade of experience, reviewed digital images of all radiographs using a standardised interpretation form (Appendix A). The interpretation form was developed by the authors (including three board-certified radiologists) based on the Fleischner Society's terms for thoracic imaging [14] and the Chest Radiograph Reading and Recording System (CRRS), that had been previously validated [15]. Although CRRS has recently been validated in patients with advanced HIV [16], we modified CRRS prior to this, to add descriptive modifiers that we thought important in describing radiographs in HIV-infected patients (*e.g.* reticular opacities commonly seen in *Pneumocystis* pneumonia). Together, the radiologists evaluated the quality of each film, and films that were technically inadequate were excluded. They involved a third radiologist (RO) to adjudicate whenever there were differences in interpretation, and differences were resolved by consensus. Radiologists were blinded to all clinical and laboratory data, and to the final diagnosis.

Data analysis

We performed bivariate analyses to describe the association between clinical variables and a confirmed microbiological diagnosis of TB. For those with TB and those without, we determined stratum-specific means or medians for continuous variables, and proportions for categorical variables. We compared them using the *t*-test or Wilcoxon rank-sum (Mann–Whitney) test for continuous variables, and the χ^2 test or Fisher's exact test for proportions. To compare proportions, we calculated risk ratios (RRs) with 95% confidence intervals. All tests were two-tailed and we considered p-values <0.05 statistically significant. Although the sample size arose from convenience, we determined the precision of all diagnostic accuracy estimates using exact binomial confidence intervals in lieu of power calculations [17]. Data were analysed using STATA IC/10 (STATA Corporation, College Station, TX).

Table 1. Demographic and clinical characteristics, stratified by TB status

Characteristic	TB[a] (n=214), n (%)	Non-TB (n=189), n (%)	p-value
Female (%)	106 (50)	100 (53)	0.50
Median age (IQR), years	33 (28–40)	35 (29–44)	0.18
HIV seropositivity (%)	186 (87)	148 (78)	0.02
Median CD4 cells mm^{-3} (IQR)	40 (12–96)	64 (23–208)	0.002
Fever or night sweats (%)	200 (93)	175 (93)	0.73
Weight loss (%)	207 (97)	172 (91)	0.02
Taking ART (%)	25 (12)	24 (13)	0.76
Received antibiotics[b] (%)	145 (69)	115 (64)	0.28
Ever smoked (%)[c]	60 (28)	51 (27)	0.81

ART, antiretroviral therapy; HIV, human immunode ficiency virus; IQR, interquartile range; TB, tuberculosis.
[a]''TB'' was defined microbiologically based on a positive smear or a positive culture on any respiratory specimen.
[b]Prior to hospital admission.
[c]''Ever smoked'' was defined as any history of smoking for >3 months and included those currently smoking.

Ethics approval

The Makerere University Research Ethics Committee, the Committee on Human Research, the Mulago Hospital Institutional Review Board and the Uganda National Council for Science and Technology approved the protocol. Some of these patients have been previously included in published studies [18–20].

Results

A total of 408 patients met inclusion criteria and underwent chest radiography. We excluded five patients whose radiographs were unreadable. Of the remaining 403 patients, 362 (90%) had radiographs of high or acceptable quality and 41 (10%) of poor quality, because of underinflation or overpenetration.

Median age was 34 years [interquartile range (IQR) 28–42]. 83% were HIV infected. Most had advanced acquired immunodeficiency syndrome (AIDS), with a median CD4+ T-cell count of 50 cells mm^{-3} (IQR 14–150 cells mm^{-3}), reflecting that 164 (50%) out of 326 patients with this information available had a CD4 T-cell count below 50 cells mm^{-3}. Of 334 HIV-infected patients, 49 (15%) were on antiretroviral therapy at the time of presentation. TB was the most common diagnosis, affecting 214 (53%) patients. 204 were culture positive, and 10 were smear positive, culture negative. 32 (8%) patients were diagnosed with culture-negative TB after responding to empiric TB treatment. Other diagnoses included bacterial pneumonia (n=61, 15%), cryptococcal pneumonia (n=6, 1%), PKS (n=4, 1%) and PCP (n=3, 1%). 8 (2%) patients had another non-infectious illness, and 62 (15%) patients did not have a final diagnosis. 13 (3%) patients had more than 1 final diagnosis. Of those, seven patients had culture-positive TB and another diagnosis (three cryptococcal pneumonia, three aspergillus infection and one PKS).

There were statistically significant but clinically small differences in the frequency of HIV seropositivity and weight loss between TB and non-TB patients: TB patients were more likely to be HIV seropositive (87% *vs* 78%, p=0.02) and to have a lower CD4+ T-cell count (median 40 cells mm^{-3} *vs* 64 cells mm^{-3}, p=0.002) than patients without TB. TB patients reported more weight loss (97% *vs* 91%, p=0.02) than non-TB cases (Table 1). There were no other significant differences between the TB and non-TB patients in terms of gender, age, presence of fever or night sweats, use of antiretroviral therapy or antibiotics, or smoking.

Table 2 compares radiographic findings between TB and non-TB patients. TB patients were less likely to have normal CXRs [12% *vs* 20%, RR 0.62, 95% confidence interval (CI) 0.39–0.98, p=0.04] and more likely to have reticulonodular opacities (45% *vs* 12%, RR 3.85, 95% CI 2.53–5.87, p<0.001), cavities (18% *vs* 7%, RR 2.58, 95% CI 1.42–4.70, p=0.001) and nodules (14% *vs* 6%, RR 2.28, 95% CI 1.21–4.31, p=0.008) than non-TB patients (Figure 1a,b). A diffuse parenchymal pattern was also

Table 2. Chest radiographic patterns in TB and non-TB patients

Radiographic findings	TB[a] (n=214), n (%)	Non-TB (n=189), n (%)	Risk ratio (95% CI)	p-value
Normal chest radiograph	26 (12)	37 (20)	0.62 (0.39–0.98)	0.04
Focal upper lobe opacities	31 (14)	23 (12)	1.19 (0.72–1.97)	0.50
Diffuse opacities	140 (75)[b]	90 (60)[c]	1.25 (1.07–1.46)	0.003
Consolidation	98 (46)	74 (39)	1.17 (0.93–1.47)	0.18
Reticulonodular opacities	96 (45)	22 (12)	3.85 (2.53–5.87)	<0.001
Cavities	38 (18)	13 (7)	2.58 (1.42–4.70)	0.001
Nodules	31 (14)	12 (6)	2.28 (1.21–4.31)	0.008
Miliary pattern	4 (2)	0	–	–
Intrathoracic lymphadenopathy	47 (22)	27 (14)	1.54 (1.00–2.37)	0.05
Pleural effusion	34 (16)	30 (16)	1.00 (0.64–1.57)	1.00

CI, confidence interval; TB, tuberculosis.
[a]TB was defined microbiologically based on a positive culture or a positive smear.
[b]Out of a total of 186 TB patients with available data.
[c]Out of a total of 150 non-TB patients with available data.

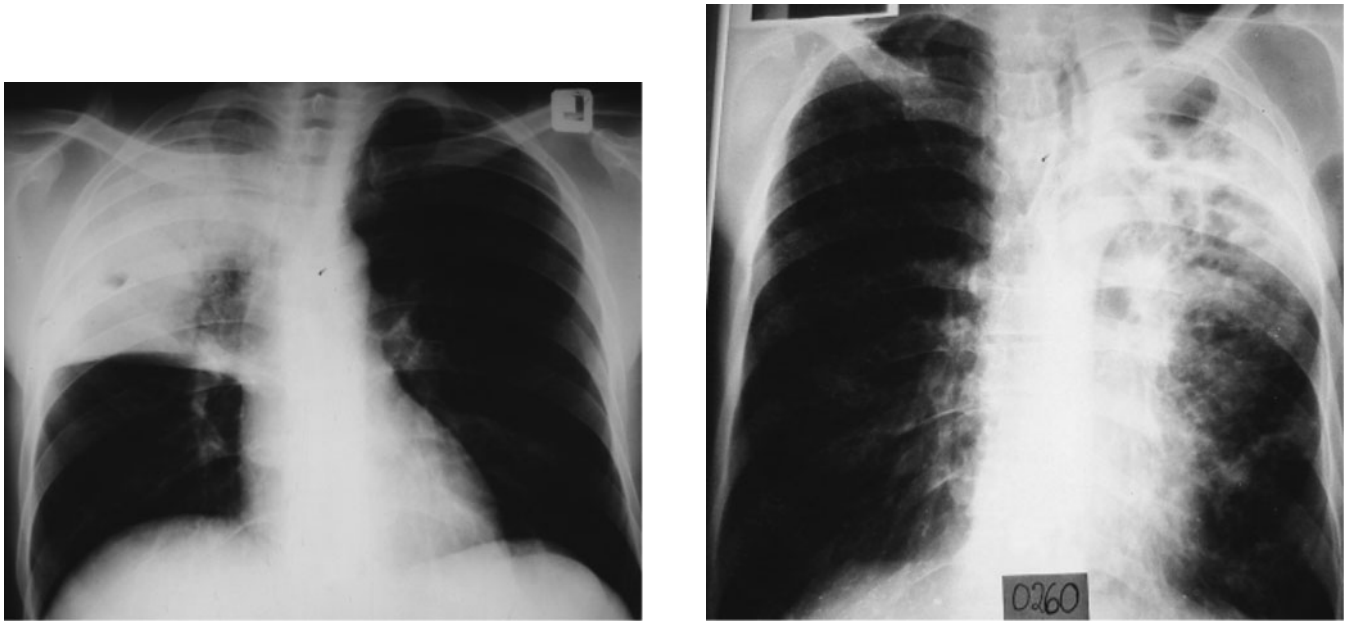

(a) (b)

Figure 1. (a) Unilobar consolidation in an human immunodeficiency virus (HIV)-seropositive patient with bacterial pneumonia. A posteroanterior chest radiograph shows homogeneous opacity with air bronchograms involving the right upper and mid zones. (b) Fibrocavitating bronchopneumonia in an HIV-seronegative patient with tuberculosis. A posteroanterior chest radiograph shows homogeneous and ring opacities in the left upper and mid zones, reticulonodular infiltrates in the left lower zones and tracheal shift to the left.

more common among TB patients (75% *vs* 60%, RR 1.25, 95% CI 1.07–1.46, $p=0.003$). All four patients with a miliary pattern had TB.

Table 3 compares radiographic findings between HIV-seropositive and HIV-seronegative TB patients. Cavities were significantly more common in HIV-seronegative TB patients than in HIV-seropositive TB patients (48% *vs* 13%, RR 3.58, 95% CI 2.10–6.12, $p<0.001$) (Figure 2a,b). Consolidation also occurred more frequently among HIV-seronegative patients (70% *vs* 42%, RR 1.66, 95% CI 1.23–2.23, $p=0.007$). All four patients with miliary abnormalities were HIV seropositive (Figure 3).

Table 4 compares radiographic findings in HIV-seropositive TB patients after stratification by CD4+ T-cell count >50 cells mm^{-3} and ≤50 cells mm^{-3}. Of 182 TB patients with CD4 cell count results, 102 (56%) had a CD4+ T-cell count ≤50 cells mm^{-3}. Patients with CD4+ T-cell counts ≤50 cells mm^{-3} had consolidation less often (33% *vs* 54%, RR 0.62, 95% CI 0.44–0.87, $p=0.006$), and more often had hilar or mediastinal lymphadenopathy (30% *vs* 16%, RR 1.87, 95% CI 1.05–3.33, $p=0.03$), than patients with a CD4+ T-cell count >50 cells mm^{-3} (Figure 4a,b). Cavities also tended to be less common in those with CD4+ T-cell counts ≤50 cells mm^{-3} (9% *vs* 19%, RR 0.47, 95% CI 0.22–1.02, $p=0.05$), although this was not statistically significant. When comparing the group of patients with CD4+ T-cell counts ≤50 cells mm^{-3} with patients who had a CD4+ T-cell count >50 but <200 cells mm^{-3} we found that patients with CD4+ T-cell counts ≤50 cells mm^{-3} had consolidation less often (33% *vs* 51%, $p=0.03$), and that there was a trend towards having more lymphadenopathy (30% *vs* 20%, $p=0.16$), than patients with a CD4+ T-cell count of 51–200 cells mm^{-3}, although this was not significant.

Table 3. Radiographic abnormalities in TB patients according to HIV status[a]

Radiographic findings	HIV– $n=27$, n (%)	HIV+ $n=186$, n (%)	Risk ratio (95% CI)	p-value
Normal chest radiograph	3 (11)	23 (12)	0.90 (0.29–2.79)	0.85
Focal upper lobe opacities	4 (15)	27 (15)	1.02 (0.39–2.69)	0.97
Diffuse opacities	17 (71)[b]	122 (76)[c]	0.93 (0.71–1.23)	0.97
Consolidation	19 (70)	79 (42)	1.66 (1.23–2.23)	0.007
Reticulonodular opacities	13 (48)	83 (45)	1.08 (0.71–1.65)	0.73
Cavities	13 (48)	25 (13)	3.58 (2.10–6.12)	<0.001
Nodules	6 (22)	25 (13)	1.65 (0.75–3.66)	0.23
Miliary pattern	0	4 (2)	0	--
Intrathoracic lymphadenopathy	3 (11)	44 (24)	0.47 (0.16–1.41)	0.14
Pleural effusion	5 (19)	28 (15)	1.23 (0.52–2.91)	0.64

CI, confidence interval; HIV, human immunodeficiency virus; TB, tuberculosis.
[a]HIV status unknown for one TB patient.
[b]Out of 24 HIV-negative patients with available data.
[c]Out of 161 HIV-positive patients with available data.

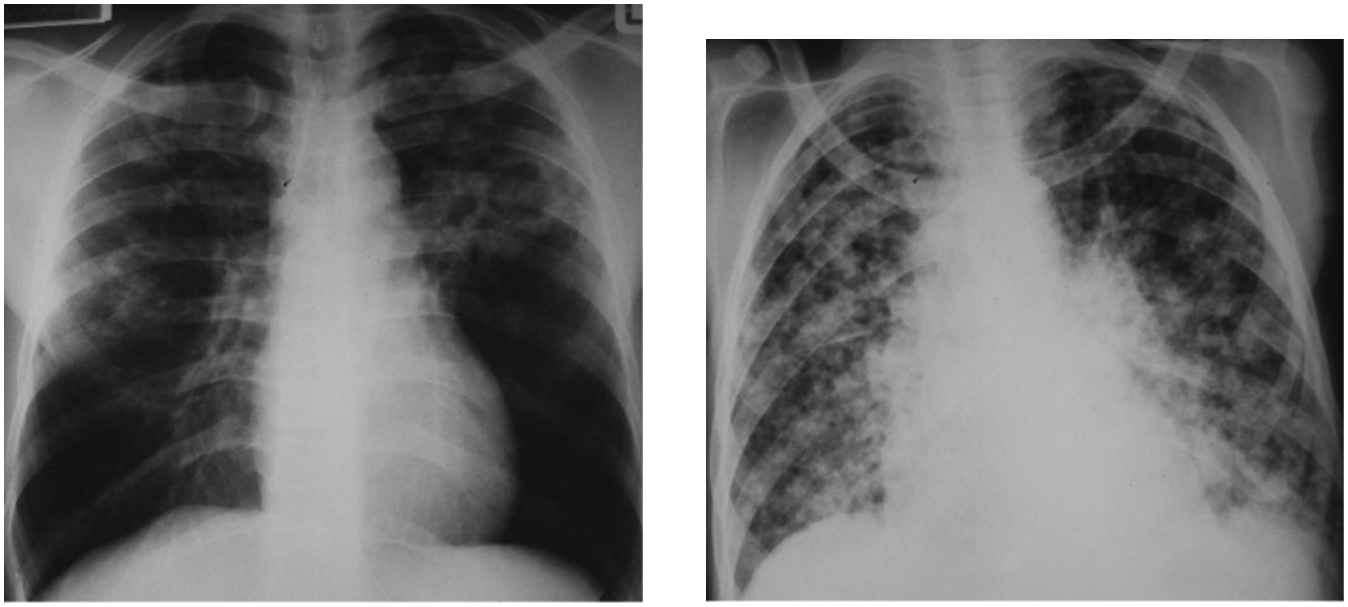

(a) (b)

Figure 2. (a) Human immunodeficiency virus (HIV)-seronegative patient with tuberculosis (TB) and cavitary bronchopneumonia. A posteroanterior chest radiograph shows patchy opacities in the upper and mid zones bilaterally and a thick-walled ring shadow in the left mid zone. (b) HIV-seropositive TB patient with a CD4+ T-cell count of 17 cells mm^{-3} and extensive bronchopneumonia. Anteroposterior chest radiograph shows bilateral diffuse reticulonodular and patchy opacities involving all lung zones.

Discussion

In the present study, we show that typical radiographic findings of TB (such as cavities, nodules and reticulonodular opacities) are still useful for differentiating TB from other pneumonias in a population with a high prevalence of HIV infection. We have also demonstrated that a lack of consolidation and a lack of cavities are the radiographic features that may be considered to define an atypical presentation since that is more common in HIV-seropositive than in HIV-seronegative patients, and in patients with advanced immunosuppression than in those with less immunosuppression.

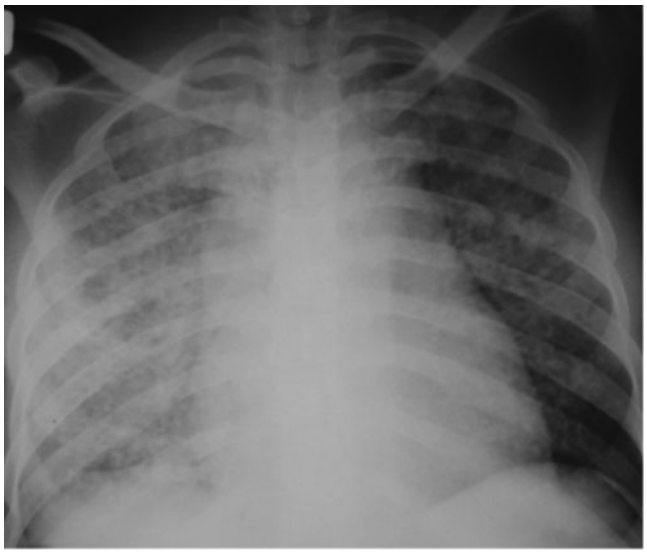

Figure 3. Miliary tuberculosis in a patient with a CD4+ T-cell count of 4 cells mm^{-3}. Anteroposterior chest radiograph shows innumerable small discrete nodules 1–2 mm in diameter, diffusely distributed throughout both lungs.

Although previous studies have described atypical patterns as being more common in HIV-infected TB patients with CD4+ T-cell counts $\leq$200 cells mm^{-3}, few have described CXR patterns of patients with CD4+ T-cell counts $\leq$50 cells mm^{-3}. For the hospitalised patients with advanced AIDS who were included in our study, immediate diagnosis and treatment are crucial in preventing deaths and the CXR has a crucial role in guiding management. Our findings confirm the atypical pattern of pulmonary TB in HIV-seropositive patients with low CD4+ T-cell counts, most importantly the absence of cavities [4, 8, 13, 21–26]. Our finding that consolidation was more common in the HIV-seronegative patient group corresponds with one prior study [6].

Although CXR is neither sufficiently sensitive nor specific for diagnosis of TB, strong radiographic associations with microbiological diagnoses exist [27] and, when combined with other available clinical and laboratory information, CXR information may influence early empiric initiation of therapy, with or without additional confirmatory testing. When interpreting CXRs, radiologists working in areas with a high prevalence of HIV-related TB should consider the way HIV status and degree of immunosuppression change the radiographic presentation, and clinicians ordering CXRs should provide radiologists with clinical and immunological information to facilitate more accurate diagnosis for TB. Better communication between clinicians and radiologists may thereby help decrease time to initiation of therapy in smear-negative patients.

Table 4. Abnormalities in HIV-seropositive TB patients according to CD4 count[a]

Radiographic findings	CD4 ≤50 cells mm^{-3} (n=102), n (%)	CD4 >50 cells mm^{-3} (n=80), n (%)	Risk ratio (95% CI)	p-value
Normal chest radiograph	14 (14)	8 (10)	1.37 (0.61–3.11)	0.44
Focal upper lobe opacities	15 (15)	11 (14)	1.07 (0.52–2.20)	0.86
Diffuse opacities	66 (77)[b]	54 (75)[c]	1.02 (0.86–1.22)	0.80
Consolidation	34 (33)	43 (54)	0.62 (0.44–0.87)	0.006
Reticulonodular opacities	41 (40)	40 (50)	0.80 (0.58–1.11)	0.19
Cavities	9 (9)	15 (19)	0.47 (0.22–1.02)	0.05
Nodules	14 (14)	10 (13)	1.10 (0.52–2.34)	0.81
Miliary pattern	3 (3)	1 (1)	2.35 (0.25–22.19)	0.63
Intrathoracic lymphadenopathy	31 (30)	13 (16)	1.87 (1.05–3.33)	0.03
Pleural effusion	14 (14)	14 (18)	0.78 (0.40–1.55)	0.48

CI, confidence interval; HIV, human immunodeficiency virus; TB, tuberculosis.
[a]CD4 count unknown for four HIV-positive TB patients.
[b]Out of 86 patients with CD4 counts ≤50 and data available.
[c]Out of 72 patients with CD4 counts >50 and data available.

One of the strengths of our study is that we used a standardised interpretation form that was developed according to recommended guidelines for interpreting CXRs. Furthermore, we used paired readings by two radiologists who, for study purposes, were blinded to clinical information. Additionally, we carried out our study in a highly relevant clinical population of admitted patients with chest symptoms from a population with a high prevalence of both HIV and TB.

There were limitations to this study. First, the resolution of the CXRs could have been compromised by digitising the images. We tried to obtain the highest quality images by standardising the way the digital photos were taken. A recently published study investigating the diagnostic accuracy of photographed radiographs for low-cost teleradiology found that there was no statistical difference between the readings from the original films and the digital images, showing that high-quality digital images do not compromise the quality of reading [28]. Second, mixed respiratory infections may influence the pattern of abnormalities seen on the radiographs. However, this is a common, well-recognised dilemma for radiologists evaluating films from immunocompromised patients. Third, 10% of the radiographs were of poor quality because of underinflation or overpenetration, issues that made accurate interpretation more difficult. Nevertheless, since these films were taken under routine conditions in a busy public referral hospital, the film quality reflects the standard quality of radiographs in clinically relevant

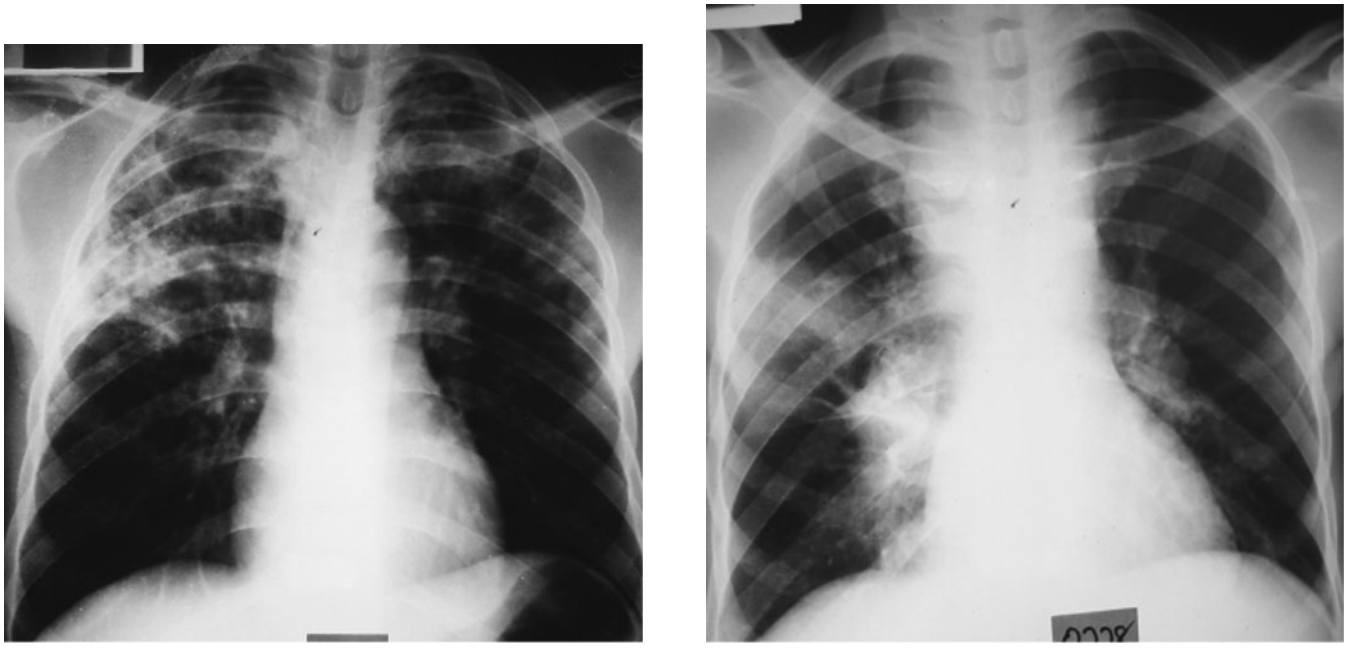

(a) (b)

Figure 4. (a) Human immunodeficiency virus (HIV)-seropositive patient with a CD4+ T-cell count of 173 cells mm^{-3} and tuberculosis (TB). A posteroanterior chest radiograph shows patchy opacities in the upper and mid zones bilaterally. (b) HIV-seropositive patient with TB and a CD4+ T-cell count of 1 cell mm^{-3}. A posteroanterior chest radiograph shows enlarged right paratracheal, tracheobronchial and bilateral hilar lymph nodes and a homogeneous opacity in the right mid zone, giving a pattern similar to a primary TB.

settings. Furthermore, it raises the possibility that quality assurance interventions could improve the usefulness of radiography in these settings. Lastly, our study was limited in size and large studies of patients across a range of CD4+ T-cell counts, including patients with a greater frequency of non-TB opportunistic conditions, are needed in order to determine what features distinguish TB from other processes in similar populations.

In conclusion, in populations highly endemic for HIV–TB coinfection, the radiographic features of TB in patients with HIV differ from the typical patterns seen in non-immunosuppressed or less immunosuppressed individuals. We found that different chest radiographic patterns may be seen in TB and non-TB pneumonia, although those differences may be especially subtle in HIV-seropositive patients and patients with very low CD4+ T-cell counts. Diffuse opacities, reticulonodular opacities, nodules or cavities point more to TB than non-TB pneumonia, but normal CXRs are less likely in TB patients. Furthermore, consolidation and cavities are less common among HIV-seropositive than among HIV-seronegative TB patients and hilar/mediastinal lymphadenopathy occur more in TB patients with CD4+ T-cell counts of ≤ 50 cells mm^{-3}. The presentation of clinical and immunological information to the radiologists interpreting the radiographs, and the assurance that the radiograph is of good quality, thus might facilitate more accurate diagnosis of TB.

Acknowledgments

This study was financially supported by grant numbers K24 HL087713 (LH), R01 HL090335 (LH), F32 HL088990 (JLD), K23 A1080147 (JLD), and K23HL094141 (AC) from the NationalInstitutes of Health. This work was also supported by the National Center for Research Resources (KL2 RR024130).

The authors thank the patients who participated in this study, and the team which enrolled them, including Florence Nankya, Rachel Kyeyune, John Kiidha, Patrick Byanyima and Kate Nabakiibi. We would also like to thank the Mulago Hospital Administration for facilitating this research, and the Infectious Diseases Research Collaboration, especially Geoff Lavoy and Joseph Kasule for their assistance with data management. We thank Robert Miller for his critical reading of the manuscript. Special thanks to Associate Professor Kiguli-Malwadde Elsie, Head of the Department of Radiology, and all of the radiographers who took the chest radiographs.

References

1. Dowdy DW, O'Brien MA, Bishai D. Cost-effectiveness of novel diagnostic tools for the diagnosis of tuberculosis. Int J Tuberc Lung Dis 2008;12:1021–9.
2. Keeler E, Perkins MD, Small P, Hanson C, Reed S, Cunningham J, et al. Reducing the global burden of tuberculosis: the contribution of improved diagnostics. Nature 2006;444:49–57.
3. World Health Organization. Improving the diagnosis and treatment of smear-negative pulmonary and extrapulmonary tuberculosis among adults and adolescents. Recommendations for HIV-prevalent and resource-constrained settings. Geneva, Switzerland: WHO; 2006.
4. Awil PO, Bowlin SJ, Daniel TM. Radiology of pulmonary tuberculosis and human immunodeficiency virus infection in Gulu, Uganda. Eur Respir J 1997;10:615–18.
5. Johnson JL, Vjecha MJ, Okwera A, Hatanga E, Byekwaso F, Wolski K, et al. Impact of human immunodeficiency virus type-1 infection on the initial bacteriologic and radiographic manifestations of pulmonary tuberculosis in Uganda. Makerere University-Case Western Reserve University Research Collaboration. Int J Tuberc Lung Dis 1998;2:397–404.
6. Lawn SD, Evans A J, Sedgwick PM, Acheampong JW. Pulmonary tuberculosis: radiological features in West Africans coinfected with HIV. Br J Radiol 1999;72:339–44.
7. Garcia GF, Moura AS, Ferreira CS, Rocha MO. Clinical and radiographic features of HIV-related pulmonary tuberculosis according to the level of immunosuppression. Rev Soc Bras Med Trop 2007;40:622–6.
8. Kawooya VK, Kawooya M, Okwera A. Radiographic appearances of pulmonary tuberculosis in HIV-1 seropositive and seronegative adult patients. East Afr Med J 2000;77:303–7.
9. Tshibwabwa ET, Richenberg JL, Aziz ZA. Lung radiology in the tropics. Clin Chest Med 2002;23:309–28.
10. Tshibwabwa ET, Mwaba P, Bogle-Taylor J, Zumla A. Four-year study of abdominal ultrasound in 900 Central African adults with AIDS referred for diagnostic imaging. Abdom Imaging 2000;25:290–6.
11. Long R, Maycher B, Scalcini M, Manfreda J. The chest roentgenogram in pulmonary tuberculosis patients seropositive for human immunodeficiency virus type 1. Chest 1991;99:123–7.
12. Louie JK, Chi NH, Thao le TT, Quang VM, Campbell J, Chau NV, et al. Opportunistic infections in hospitalized HIV-infected adults in Ho Chi Minh City, Vietnam: a cross-sectional study. Int J STD AIDS 2004;15:758–61.
13. Post FA, Wood R, Pillay GP. Pulmonary tuberculosis in HIV infection: radiographic appearance is related to CD4+ T-lymphocyte count. Tuber Lung Dis 1995;76:518–21.
14. Hansell DM, Bankier AA, MacMahon H, McLoud TC, Müller NL, Remy J. Fleischner Society: glossary of terms for thoracic imaging. Radiology 2008;246:697–722.
15. den Boon S, Bateman ED, Enarson DA, Borgdorff MW, Verver S, Lombard CJ, et al. Development and evaluation of a new chest radiograph reading and recording system for epidemiological surveys of tuberculosis and lung disease. Int J Tuberc Lung Dis 2005;9:1088–96.
16. Dawson R, Masuka P, Edwards DJ, Bateman ED, Bekker LG, Wood R, et al. Chest radiograph reading and recording system: evaluation for tuberculosis screening in patients with advanced HIV. Int J Tuberc Lung Dis 2010;14:52–8.
17. Cummings P, Rivara FP. Reporting statistical information in medical journal articles. Arch Pediatr Adolesc Med 2003; 157:321–4.
18. Cattamanchi A, Davis JL, Worodria W, den Boon S, Yoo S, Matovu J, et al. Sensitivity and specificity of fluorescence microscopy for diagnosing pulmonary tuberculosis in a high HIV prevalence setting. Int J Tuberc Lung Dis 2009; 13:1130–6.
19. Cattamanchi A, Dowdy DW, Davis JL, Worodria W, Yoo S, Joloba M, et al. Sensitivity of direct versus concentrated sputum smear microscopy in HIV-infected patients suspected of having pulmonary tuberculosis. BMC Infect Dis 2009;9:53.
20. Cattamanchi A, Davis JL, Worodria W, Yoo S, Matovu J, Kiidha J, et al. Poor performance of universal sample processing method for diagnosis of pulmonary tuberculosis by smear microscopy and culture in Uganda. J Clin Microbiol 2008;46:3325–9.
21. Barnes PF, Bloch AB, Davidson PT, Snider DE Jr. Tuberculosis in patients with human immunodeficiency virus infection. N Engl J Med 1991;324:1644–50.
22. Cecconi L, Busi Rizzi E. Diagnostic imaging: mycobacteriosis and human immunodeficiency virus (HIV) infection. Rays 1994;19:127–41.

23. Davis SD, Yankelevitz DF, Williams T, Henschke C. Pulmonary tuberculosis in immunocompromised hosts: epidemiological, clinical, and radiological assessment. Semin Roentgenol 1993;28:119–30.
24. Keiper MD, Beumont M, Elshami A, Langlotz CP, Miller WT Jr. CD4 T lymphocyte count and the radiographic presentation of pulmonary tuberculosis. A study of the relationship between these factors in patients with human immunodeficiency virus infection. Chest 1995;107: 74–80.
25. Goodman PC. Tuberculosis and AIDS. Radiol Clin North Am 1995;33:707–17.
26. Shah RM, Kaji AV, Ostrum BJ, Friedman AC. Interpretation of chest radiographs in AIDS patients: usefulness of CD4 lymphocyte counts. Radiographics 1997;17:47–58; discussion 59–61.
27. Tattevin P, Casalino E, Fleury L, Egmann G, Ruel M, Bouvet E. The validity of medical history, classic symptoms, and chest radiographs in predicting pulmonary tuberculosis: derivation of a pulmonary tuberculosis prediction model. Chest 1999;115:1248–53.
28. Szot A, Jacobson FL, Munn S, Jazayeri D, Nardell E, Harrison D, et al. Diagnostic accuracy of chest X-rays acquired using a digital camera for low-cost teleradiology. Int J Med Inform 2004;73:65–73.

Appendix A

FORM 9: MIND STUDY
CHEST RADIOGRAPH INTERPRETATION DATA

				''.'' if N/A
0. a. Date_____/_____/_____				0a.
b. What is the overall quality of the film?				0b.
HIGH	0	POOR	2	
ACCEPTABLE	1	UNREADABLE	3	

1. Does the parenchyma appear abnormal? 1.
NO 0 (Go to #12)
YES 1 (Go to #2)

2–7. Please describe the infiltrate in each of the following zones using the following codes:

a. Pattern
Normal 0
Mass 1
Reticulolinear 2
Reticulonodular 3
Nodules 4
Ring opacity 5
Ground glass 6
Consolidation 7
Hyperlucent 8
Linear band 9
Pleural opacity 10
Mixed (specify e) 11
Other (specify f) 12

Fill only if the answer for ''a. Pattern'' is…
11
b. Mixed
(List patterns using + sign; e.g. 2+3+4)
12
c. Other

	a.	b.	c.
2. RU lung zone	a.	b.	c.
3. RM lung zone	a.	b.	c.
4. RL lung zone	a.	b.	c.
5. LU lung zone	a.	b.	c.
6. LM lung zone	a.	b.	c.
7. LL lung zone	a.	b.	c.

		''.'' if N/A
8. Consolidation		8.
HOMOGENEOUS	0	
PATCHY	1	
9. Nodule details (Specify only if answer to questions 2–7 includes ''4'')		
a. Number		9a.
SOLITARY	0	
MULTIPLE	1	
b. Size		9b.
MILIARY (<2 mm)	0	
SMALL (2–3 mm)	1	
MEDIUM (>3–5 mm)	2	
LARGE (>5 mm)	3	
c. Calcification		9c.
NON-CALCIFIED	0	
CALCIFIED	1	
BOTH	2	

10. Cavity details (Specify only if answer to questions 2–7 includes ''5'')		
a. Number		10a.
SOLITARY	0	
MULTIPLE	1	
b. Size		10b.
SMALL (<2 cm)	1	
MEDIUM (2–5 cm)	2	
LARGE (>5 cm)	3	
c. Wall thickness		10c.
THIN (≤1 mm)	0	
MODERATE (1–3 mm)	1	
MARKED (>3 mm)	2	
d. Fluid levels		10d.
ABSENT	0	
PRESENT	1	
e. Intracavitary bodies		10e.
ABSENT	0	
PRESENT	1	
11. Predominant location of the findings on the radiograph as a whole?		
a. Distribution		11a.
FOCAL DISEASE	0	
DIFFUSE DISEASE	1	
b. If focal disease		11b.
UPPER LOBE	0	
MIDDLE LOBE	1	
LOWER	2	
c. Centrality of diffuse		11c.
CENTRAL	0	
PERIPHERAL	1	
UNIFORM	2	
d. Symmetry		11d.
BOTH	0	
RIGHT	1	
LEFT	2	
12. Cardiac silhouette		12.
NORMAL	0	
ENLARGED	1	
UNINTERPRETABLE	2	
13. Mediastinal position		13.
MIDLINE	0	
SHIFTED RIGHT	1	
SHIFTED LEFT	2	
14. Mediastinal size		14.
NORMAL	0	
WIDENED	1	
MASS	2	
15. Hilar elevation		15.
NONE	0	
RIGHT	1	
LEFT	2	
BOTH	3	
16. Is hilar/mediastinal lymphadenopathy present?		16.
NO	0 (Go to 17)	
YES	1 (Go to 16a)	
a. Location?		16a.
BOTH	0	
RIGHT	1	
LEFT	2	
17. Pleural abnormalities		
a. Apical cap?		17a.
NO	0	
YES	1	
RIGHT	1	
LEFT	2	
BOTH	3	
c. Effusion		17c.
ABSENT	0 (Go to 18)	
RIGHT	1 (Go to 17d)	

LEFT	2 (Go to 17d)	
BOTH	3 (Go to 17d)	
d. Effusion size		17d.
SMALL (Less than one lung zone)	0	
MODERATE (between 1 and 2 lung zones)	1	
MASSIVE (>2 lung zones)	2	
e. Effusion type		17e.
FREE	0	
LOCULATED	1	
f. Pneumothorax		17f.
ABSENT	0 (Go to 18)	
RIGHT	1 (Go to 17g)	
LEFT	2 (Go to 17g)	
BOTH	3 (Go to 17g)	
g. Pneumothorax size		17g.
SMALL (less than 1/3 of the hemithorax)	0	
MODERATE (2/3 of hemithorax)	1	
MASSIVE (>2/3 of hemithorax)	2	
18. Radiological extent of disease:		18.
NORMAL	0	
MINIMAL	1	
MODERATELY ADVANCED	2	
FAR ADVANCED	3	
19. Radiological impression of parenchyma		19.
Normal parenchyma	0	
Lobar pneumonia	1	
Bronchopneumonia	2	
Interstitial pneumonia	3	
Collapse/atelectasis	4	
Fibrosis	5	
Fibrocavitary pneumonia	6	
Cavitary pneumonia	7	
Miliary TB pattern	8	
Solitary pulmonary nodule	9	
Mass	10	
Emphysema	11	
Pleural effusion/disease	12	
Pneumothorax	13	
Pulmonary cardiovascular disease	14	
Bronchiectasis	15	
Others, specify	16	
20. Likelihood of TB		20.
Probable (findings consistent with TB)	0	
Possible (atypical findings)	1	
Unlikely (findings not consistent with TB)	2	
Unable to assess	3	
21. Radiological diagnosis		21.
Normal	0	
Pulmonary tuberculosis	1	
Extrapulmonary tuberculosis	2	
Bacterial pneumonia	3	
Pneumocystis pneumonia	4	
Pulmonary Kaposi's sarcoma	5	
Lymphoma	6	
Lymphocytic interstitial pneumonia	7	
Other	8 (Specify in 21a)	
a. Specify other _____		
22. Radiologist		22.
OR/HNK	0	
HNK/MK	1	
OR/MK	2	